NEURAL REGENERATION RESEARCH
www.nrronline.org

Research Article

DL-3-n-butylphthalide alleviates motor disturbance by suppressing ferroptosis in a rat model of Parkinson's disease

Chun-Bo Hu[1, 2, #], Hui Jiang[2, #], Yin Yang[1], Guo-Hua Wang[2], Qiu-Hong Ji[1], Zhong-Zheng Jia[3], Li-Hua Shen[1, *], Qian-Qian Luo[2, *]

https://doi.org/10.4103/1673-5374.343892
Date of submission: November 26, 2021
Date of decision: January 21, 2022
Date of acceptance: February 24, 2022
Date of web publication: April 25, 2022

From the Contents

Graphical Abstract

Neuroprotective effects of DL-3-n-butylphthalide in a rotenone-induced rat model of PD

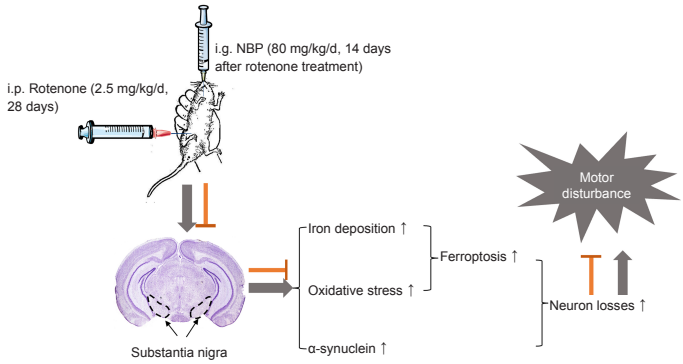

Abstract

DL-3-n-butylphthalide (NBP)—a compound isolated from Apium graveolens seeds—is protective against brain ischemia via various mechanisms in humans and has been approved for treatment of acute ischemic stroke. NBP has shown recent potential as a treatment for Parkinson's disease. However, the underlying mechanism of action of NBP remains poorly understood. In this study, we established a rat model of Parkinson's disease by intraperitoneal injection of rotenone for 28 successive days, followed by intragastric injection of NBP for 14–28 days. We found that NBP greatly alleviated rotenone-induced motor disturbance in the rat model of Parkinson's disease, inhibited loss of dopaminergic neurons and aggregation of α-synuclein, and reduced iron deposition in the substantia nigra and iron content in serum. These changes were achieved by alterations in the expression of the iron metabolism-related proteins transferrin receptor, ferritin light chain, and transferrin 1. NBP also inhibited oxidative stress in the substantia nigra and protected mitochondria in the rat model of Parkinson's disease. Our findings suggest that NBP alleviates motor disturbance by inhibition of iron deposition, oxidative stress, and ferroptosis in the substantia nigra.

Key Words: cystine/glutamate antiporter solute carrier family 7 member 11; DL-3-n-butylphthalide; ferritin light chain; ferroportin 1; ferroptosis; glutathione peroxidase 4; oxidative stress; iron; rotenone; transferrin receptor

Introduction

Parkinson's disease (PD) is a neurodegenerative disease that commonly occurs in older adult people. Patients with PD usually have symptoms such as quiescent tremor, motor delay, myotonia, and postural balance disorders (Liaw et al., 2005; Bloem et al., 2021). The pathological features of PD include the loss of dopamine (DA) neurons, iron deposition, and the formation of Lewy bodies, which mainly comprise α-synuclein (α-syn) aggregations (Spillantini et al., 1997; Duda et al., 2000; Dorszewska et al., 2021) in the substantia nigra (SN) pars compacta. However, the pathogenesis of PD is still unclear. Many studies have shown that excessive unstable iron in the SN results in oxidative stress and generates reactive oxygen species (ROS) through the Fenton reaction (Chen et al., 2019b; Angelova et al., 2020; Han et al., 2021). According to observations of patients with PD, excess iron and oxidative stress are important factors in ferroptosis (Do Van et al., 2016). In addition, ferroptosis is associated with pathogenic changes found in PD animal models, such as elevated iron deposits in the SN, consumed glutathione (GSH), lipid peroxidation, and increased generation of ROS (Dias et al., 2013; Stockwell et al., 2017; Gao et al., 2019). Therefore, it is important to identify potential therapeutic strategies to prevent iron deposition and ferroptosis during the development of PD.

DL-3-n-butylphthalide (NBP) is a compound that is isolated from Apium graveolens seeds. To date, NBP has been approved by the National Medical Products Administration to treat acute ischemic stroke (Xu et al., 2019b). NBP exerts protective effects on brain ischemia via various mechanisms, including antithrombosis, antiapoptosis, and antioxidation activities, protection of mitochondria, and promotion of angiogenesis (Tian et al., 2017; Wang et al., 2018b). Previous studies have shown that the therapeutic role of NBP is not confined to cerebrovascular disease and that NBP protects dopaminergic neurons in a rotenone model of PD (Xiong et al., 2012a; Chen et al., 2018). However, the mechanism of action of NBP for the treatment of PD is not fully understood.

Rotenone is a naturally occurring compound that originates from the roots of the Derris and Lonchocarpus plant species (Jenner, 2001) and has been used as an inhibitor of mitochondrial complex I to establish PD animal models since the 1980s (Heikkila et al., 1985). Rotenone can induce α-syn accumulation and the subsequent generation of Lewy body-like inclusion bodies, resulting in the selective degeneration of dopaminergic neurons in the SN (Betarbet et al., 2000; Deng et al., 2021). In this study, we aimed to investigate the neuroprotective effects and mechanism of action of NBP in a rotenone-induced rat model of PD.

[1]Department of Neurology, Affiliated Hospital of Nantong University, Nantong, Jiangsu Province, China; [2]Department of Physiology and Hypoxic Biomedicine, Institute of Special Environmental Medicine and Co-innovation Center of Neuroregeneration, Nantong University, Nantong, Jiangsu Province, China; [3]Department of Medical Imaging, Affiliated Hospital of Nantong University, Nantong, Jiangsu Province, China
*Correspondence to: Li-Hua Shen, MD, PhD, lihuashennt@126.com; Qian-Qian Luo, PhD, qianqianluo@ntu.edu.cn.
https://orcid.org/0000-0001-8302-3117 (Qian-Qian Luo)
#Both authors contributed equally to this work.

Funding: *This work was funded by the National Natural Science Foundation of China, No. 81873924 (to QQL), No. 82171190 (to GHW); Nantong Science and Technology Project of China, No. MS22021010 (to LHS); and High-level Innovation and Entrepreneurship Talents Introduction Program of Jiangsu Province of China (to QQL).*
How to cite this article: *Hu CB, Jiang H, Yang Y, Wang GH, Ji QH, Jia ZZ, Shen LH, Luo QQ (2023) DL-3-n-butylphthalide alleviates motor disturbance by suppressing ferroptosis in a rat model of Parkinson's disease. Neural Regen Res 18(1):194-199.*

Methods

Animals

The prevalence of PD is higher in men than in women (Gillies et al., 2014), and many studies have used male rats to establish PD models. Moreover, the iron levels in male rats are more stable than in female rats (Cannon et al., 2009; von Wrangel et al., 2015). Therefore, we used 60 adult male Sprague-Dawley rats (8 weeks old, 220–250 g) supplied by the Animal Experimental Center of Nantong University, Nantong, China. The rats were randomly divided into three groups: control, rotenone, and NBP groups (n = 20 for each group). The rats were housed in stainless steel cages at 55–60% relative humidity and at 21 ± 2°C with alternating 12-hour periods of light and dark. The rats were adapted to the laboratory environment for 5 days before the experiments. The body weights of the rats were measured daily in the experimental period. Rotenone (MilliporeSigma, Burlington, MA, USA, Cat# R8875) and NBP (CSPC Pharmaceutical Group Ltd., Shijiazhuang, China, Cat# H20050299) were dissolved in 99% pure sunflower oil, and the final concentrations of rotenone and NBP were 2 and 50 mg/mL, respectively. The rats in the rotenone and NBP groups received rotenone at 2.5 mg/kg once per day intraperitoneally from day 1 to day 28, and the control group received only 99% pure sunflower oil at 1.25 mL/kg once per day intraperitoneally from day 1 to day 28 (Cannon et al., 2009; Zhang et al., 2021a). The rats in the NBP group received NBP at 80 mg/kg once a day by intragastric administration from day 14 to day 28, and the rats in the rotenone and control groups were given 99% pure sunflower oil at 1.6 mL/kg from day 14 to day 28 (Zhou et al., 2019). The rats were subjected to behavioral tests and then anesthetized by intraperitoneal injection of 40 mg/kg sodium pentobarbital (Cat# P-010, MilliporeSigma). Finally, the rats were euthanized to obtain serum and SN tissues in accordance with previously published methods (Risold and Swanson, 1997). The interventions and time points are shown in **Figure 1A**. All animals were treated in accordance with the National Research Council Guide for the Care and Use of Laboratory Animals (National Research Council (US) Committee for the Update of the Guide for the Care and Use of Laboratory Animals, 2011), and the Animal Ethics Committee of Nantong University approved this study (approval No. S20210303-018) on March 3, 2021.

Behavioral tests

Rotarod test

The rats were placed on a rotarod cylinder (IITC Life Science, Woodland Hills, CA, USA), and the time the animals stayed on the rotarod was measured. We increased the speed slowly from 4 revolutions/minute to 40 revolutions/minute over 5 minutes. The test ended if the rat dropped or grasped the device from the rung and rotated continuously for two turns without attempting to walk on the rung. The rats were trained daily for 1 week before rotenone injection. Three rotarod measurements per test were used to record the latency to fall (Ding et al., 2020).

Balance beam test

A wooden stick of 1 m in length and 2.5 cm in width and with a square cross-section (Shanghai Yuyan Instruments Co. Ltd., Shanghai, China) was placed horizontally at a distance of 60 cm from the ground, and the rats were allowed to walk on the balance beam. Rats were left on the balance beam until they fell off or for a maximum of 1 minute, and the scoring was achieved across triplicate experiments. The scoring criteria included six grades: 6 points, able to jump and walk on the balance beam without falling; 5 points, able to jump and walk on the balance beam with a less than or equal to 50% chance of falling; 4 points, able to jump and walk on the balance beam with a more than 50% chance of falling; 3 points, able to walk on the balance beam with the help of the unaffected hind limb, but the affected paralyzed hind limb cannot help move the rat forward; 2 points, unable to walk but can sit on the balance beam; and 1 point, the rat falls when placed on the balance beam (Chen et al., 2001).

Foot fault test

We conducted a foot fault test in accordance with the methods of Metz and Whishaw (Metz and Whishaw, 2002). Each rat was placed on a 50 cm × 40 cm mesh screen (Shanghai Yuyan Instruments Co., Ltd.). The mesh density was 2 cm × 2 cm, and the screen was placed at a height of approximately 30 cm. The rats were pretrained daily for 7 days such that they could walk on the mesh, and the total number of steps taken by the rats and the number of normal steps taken using forelimbs and hindlimbs for 1 minute were recorded during the formal testing. We calculated the foot fault value as the number of wrong steps and falls/the number of overall steps × 100 %. For each rat, three measurements were recorded, and their average values were registered as their scores.

Immunofluorescence

Tyrosine hydroxylase (TH) is an enzyme important for DA synthesis and is a marker of dopaminergic neurons (Fujino et al., 2020). SN coronal sections (30 µm in thickness) were cut from –4.5 to –6.2 mm caudal to bregma in the frozen brain tissue by using a cryotome (Thermo Fisher Scientific) and then were blocked in Tris-buffered saline with 3% bovine serum albumin for 2 hours and incubated with a TH primary antibody (rabbit, 1:500, Abcam, Cambridge, UK, Cat# ab6211, RRID: AB_2240393) overnight. After washing with Tris-buffered saline, the secondary antibody Alexa Fluor® 488 donkey anti-rabbit IgG (1:500, Abcam, Cat# ab150073, RRID: AB_2636877) was applied to the sections for 2 hours at room temperature. 2-(4-Amidinophenyl)-6-indolecarbamidine dihydrochloride (Beyotime Biotechnology, Shanghai, China) was used to stain the nuclei for 15 minutes at room temperature, and the cells were washed with phosphate buffer solution three times. The sections were sealed with 50% glycerol, and the detection of fluorescence signals was conducted using an SP8 confocal laser scanning microscope (Leica, Wetzlar, Germany). Results are shown as TH-positive neurons in the SN.

Western blot analysis

The SN tissues were dissected from the rat brains and homogenized for 30 minutes on ice in radioimmunoprecipitation assay lysis buffer (Beyotime Biotechnology, Cat# P0013B). The harvested lysate was centrifuged for 15 minutes at 12,000 × g at 4°C, and the supernatant was used for the protein concentration analysis. The protein concentration was determined by a bicinchoninic acid protein concentration assay kit (Cat# P0010S, Beyotime Biotechnology). The proteins were denatured at 100°C for 5 minutes in a 5× loading buffer (Beyotime Biotechnology). Samples containing 20 µg protein were loaded and separated on 8–11.2% sodium dodecyl sulfate-polyacrylamide gels, and the proteins in the gel were transferred to polyvinylidene fluoride membranes (MilliporeSigma). The membranes were blocked in Tris-buffered saline with Tween-20 that contained 5% skim milk at room temperature for 2 hours. The overnight incubation of the membranes was performed with primary antibodies against α-syn (rabbit, 1:500, MilliporeSigma, Cat# SAB4502831, RRID: AB_10746736), GSH peroxidase 4 (GPX4; rabbit, 1:1000, Abcam, Cat# ab125066, RRID: AB_10973901), transferrin receptor (TfR; mouse, 1:1000, Thermo Fisher Scientific, MA, USA, Cat# 13-6800, RRID: AB_2533029), ferritin light chain (Ft-L; rabbit, 1:1000, Abcam, Cat# ab69090, RRID: AB_1523609), ferroportin 1 (Fpn1; rabbit, 1:1000, Novus, Centennial, CO, USA, Cat# NBP1-21502, RRID: AB_1660490), cystine/glutamate antiporter solute carrier family 7 member 11 (xCT; rabbit, 1:1000, Proteintech, Chicago, IL, USA, Cat# 26864-1-AP, RRID: AB_2880661), and glyceraldehyde-3-phosphate dehydrogenase (mouse, 1:10,000, MilliporeSigma, Cat# MAB374, RRID: AB_2107445) at 4°C. Horseradish peroxidase–labeled goat antirabbit (1:10,000, Bioworld Technology, Inc., Bloomington, MN, USA, Cat# BS13278, RRID: AB_2773728) or antimouse (1:10,000, Jackson ImmunoResearch Labs, Commonwealth of Pennsylvania, PA, USA, Cat# 115-035-003, RRID: AB_10015289) secondary antibodies were incubated with the membranes at room temperature for 2 hours. ImageJ 1.52 software (https://imagej.net/downloads; National Institutes of Health, Bethesda, MD, USA) (Schneider et al., 2012) was used to scan and analyze the final images. Results are shown as the optical density ratio normalized to glyceraldehyde-3-phosphate dehydrogenase.

Perls' iron staining

The rats were perfused with 4% paraformaldehyde (MilliporeSigma), and the brain was removed, fixed with 4% paraformaldehyde for 6 hours, and dehydrated by immersion in 20% sucrose and then in 30% sucrose. The whole brain tissue was sliced coronally into 30 µm thick sections on a cryotome (Thermo Fisher Scientific). The sections were fixed with 4% paraformaldehyde, washed with double distilled water for 30 seconds, and incubated in freshly prepared solutions of 2% hydrogen chloride and 2% potassium ferrocyanide (Thermo Fisher Scientific) for 30 minutes. The hydrogen chloride and potassium ferrocyanide solutions were omitted when preparing the negative control sections. The 20-minute elimination of endogenous peroxidase activity was performed with 99% methanol and 1% hydrogen peroxide (Wang et al., 2015). The diaminobenzidine reaction products were observed under a fluorescence microscope (DM4000 B, Leica), and images were captured at a final magnification of 200×. The data were collected from three fields of view per rat.

Inductively coupled plasma mass spectrometry analysis

An inductively coupled plasma mass spectrometer (ICP–MS; Agilent Technologies, Inc., Santa Clara, CA, USA, Cat# G7850) was applied to measure the levels of iron in the serum. Rat serum samples were placed in tubes; hydrogen peroxide and then 5% nitric acid were added. Nitric acid (5%) was put into another tube as a control. The mixtures were left at room temperature overnight and then were centrifuged to remove the supernatant. A standard curve from 0 to 200 µg/L iron was created to determine the iron concentration of the serum. ICP–MS was used to assess the standards, control, and digested samples in triplicate.

Transmission electron microscopy

On the basis of the outcomes of TH immunostaining, we isolated the SN of the midbrain (1 mm^3) using a stereomicroscope (Leica). The SN was fixed in fresh 2.5% glutaric dialdehyde in 0.1 M sodium chloride buffer at 4°C. After rinsing three times, the tissue blocks were placed in 2% osmium tetroxide in 2% potassium ferricyanide in 0.1 M glutaric dialdehyde at 4°C in the dark for 2 hours and then rinsed with distilled water. The tissue blocks were stained for 2 hours with 1% uranyl acetate in the dark and rinsed with distilled water. The samples were passed through increasing concentrations of ethanol over 20 minutes (30%, 50%, 70%, 80%, 90%, 95%, and 100%) for dehydration, followed by incubation for 20 minutes in a 1:1 (v/v) mixture of ethanol and acetone. Then, the samples were left in a mixture of pure acetone (20 minutes), embedding resin (Epon 812, Electron Microscopy Sciences, Hatfield, PA, USA), pure acetone (1:1 v/v for 1 hour and then 3:1 v/v for 3 hours), and pure resin. The samples were then placed in fresh resin for 2 hours, transferred to a new embedding mold, and heated in an oven at 65°C for 24–48 hours. Next, 70 nm thick sections from the resin blocks were prepared. These sections were stained for 5 minutes with lead citrate and uranyl acetate solution. Images were obtained with a Tecnai Spirit 120 kV transmission electron microscope (Thermo Fisher Scientific).

Lipid peroxidation determination

Malondialdehyde (MDA) and GSH were chosen as lipid peroxidation detection indices. The two indices were tested in the rat SN using an MDA kit (Cat# A003-1-2, Nanjing Jiancheng Bioengineering Institute, Nanjing, China) and a GSH kit (Nanjing Jiancheng Bioengineering Institute, Cat# A006-1). The optical densities at 532 nm for MDA and 420 nm for GSH were measured with a Synergy 2 microplate reader (Agilent Technologies, Inc.). Each sample were measured three times, and the average absorbance values were calculated for every sample. A standard curve of MDA and GSH were generated. The concentration of MDA and GSH in the samples was calculated using the standard curve.

Statistical analysis

No statistical methods were used to predetermine sample sizes; however, our sample sizes are similar to those reported in previous publications (Liao et al., 2009; Zhou et al., 2019). Rats that died or did not exhibit expected characteristics of the PD model were excluded from the experiments. The evaluator was blinded to groupings. The data were expressed as the mean ± standard error of the mean (SEM). One-way analysis of variance followed by Tukey's *post hoc* test was performed using GraphPad Prism version 8.0.0 for windows (GraphPad Software, San Diego, CA, USA, www.graphpad.com). The correlation was analyzed by Pearson correlation analysis. Results with $P < 0.05$ were defined as statistically significant.

Results

NBP reverses weight loss and alleviates motor disturbance induced by rotenone

We examined the potential therapeutic roles of NBP in a rotenone-induced rat model of PD. The rats were treated with rotenone and NBP (**Figure 1A**). Rotenone suppressed weight gain compared with that in control rats ($P < 0.0001$) (**Figure 1B**). In addition, rotenone significantly impaired the rats' motor abilities, as reflected by the results of the rotarod test ($P = 0.0001$; **Figure 1C**), beam balance test ($P < 0.0001$; **Figure 1D**), and foot fault test ($P < 0.0001$; **Figure 1E**). NBP treatment rescued the rotenone-induced suppression of weight gain ($P < 0.0001$) and motor disturbance ($P < 0.0001$), especially 14 days after NBP treatment (**Figure 1C–E**).

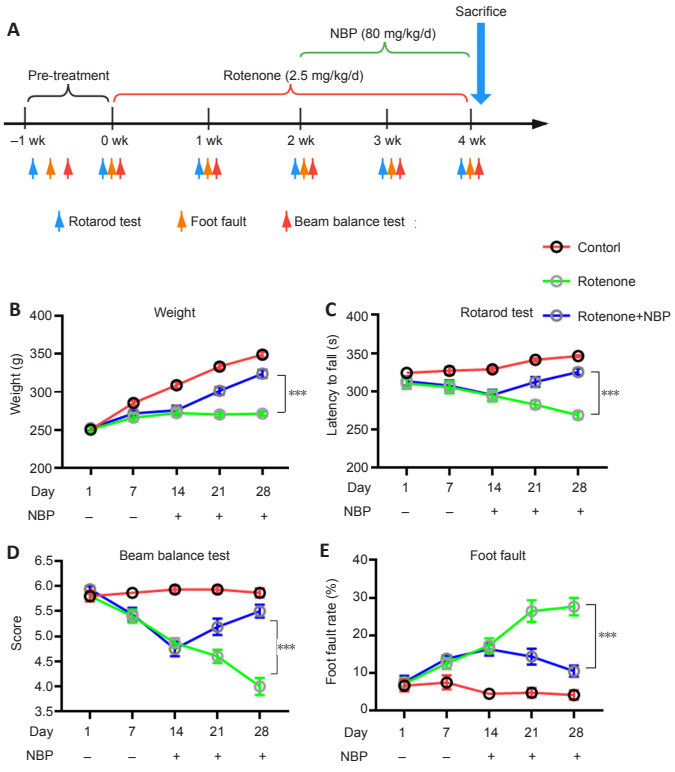

Figure 1 | NBP reverses weight loss and alleviates motor disturbance induced by rotenone.

(A) The timeline of the establishment of the rotenone-induced rat model of Parkinson's disease, and time points of the experiments. (B) NBP inhibited rotenone-induced weight loss in rats. (C–E) Quantitative results of latency to fall in the rotarod test (C), score in the beam balance test (D), and foot fault rate in the foot fault test (E). All data are shown as the mean ± SEM (n = 15–20 rats per group). ***$P < 0.001$ (one-way analysis of variance followed by Tukey's *post hoc* test). NBP: DL-3-n-butylphthalide.

NBP inhibits rotenone-induced α-synuclein overexpression and degeneration of dopaminergic neurons

We examined the role of NBP in α-syn expression and dopaminergic neuron loss in the SN in a rotenone-induced rat model of PD by measuring α-syn expression using western blot and dopaminergic neuron loss by immunostaining for TH. Our results show that rotenone induced α-syn expression in the SN compared with that in control rats ($P = 0.0003$; **Figure 2A** and **B**). However, the expression of α-syn in the SN was decreased after NBP treatment ($P = 0.0115$; **Figure 2A** and **B**). In addition, TH immunostaining showed that the proportion of TH-positive neurons in the SN of rotenone-treated rats decreased compared with those in control rats ($P < 0.0001$; **Figure 2C** and **D**). NBP treatment effectively inhibited the rotenone-induced loss of TH-positive neurons ($P < 0.0001$; **Figure 2C** and **D**).

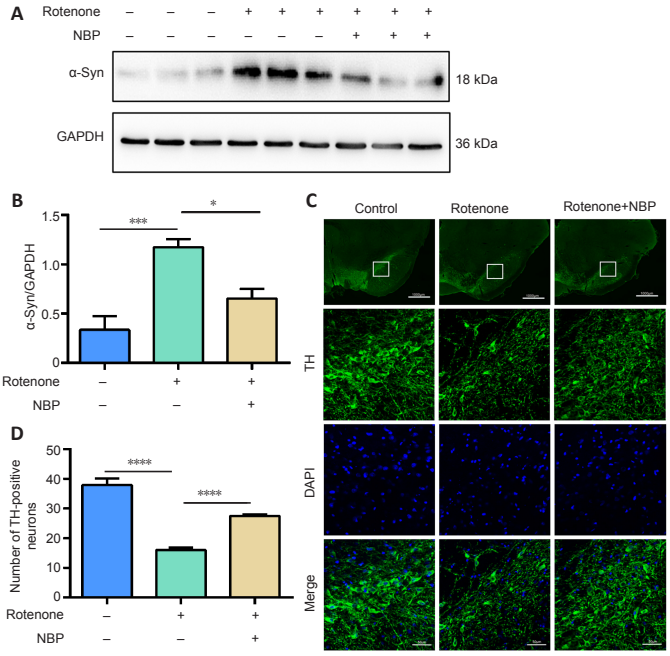

Figure 2 | NBP ameliorates the rotenone-induced loss of DA neurons and expression of α-synuclein in the substantia nigra in a rat model of Parkinson's disease.

(A) NBP suppressed the rotenone-induced increase in α-syn expression in the substantia nigra. (B) Quantitative western blot analysis of results from A. (C) NBP ameliorated the loss of TH-positive neurons induced by rotenone. Images in the second to fourth rows are magnifications of the boxed areas in the first row. Scale bars: 1000 μm (top) and 50 μm (bottom three rows). (D) Quantitative results of TH-positive neurons in the substantia nigra. All data are shown as the mean ± SEM (n = 5–9 rats per group). *$P < 0.05$, ***$P < 0.001$, ****$P < 0.0001$ (one-way analysis of variance followed by Tukey's *post hoc* test). α-syn: α-Synuclein; DA: dopaminergic; DAPI: 2-(4-amidinophenyl)-6-indolecarbamidine dihydrochloride; GAPDH: glyceraldehyde-3-phosphate dehydrogenase; NBP: DL-3-n-butylphthalide; SN: substantia nigra; TH: tyrosine hydroxylase.

NBP decreases the iron content in the substantia nigra and serum and reverses iron-related protein expression in the substantia nigra in a rat model of Parkinson's disease

To determine whether the loss of dopaminergic neurons in the rotenone-induced PD model was caused by iron overload, we examined the roles of NBP in iron deposition in the SN by Perls' iron staining and by measuring serum iron content by ICP–MS. We found that rotenone caused significant iron deposition in the SN ($P = 0.0002$; **Figure 3A** and **B**), and treatment with NBP stopped the iron deposition in the SN in the rotenone-induced rat model of PD ($P = 0.0006$; **Figure 3A** and **B**). In addition, serum iron was significantly increased in the rat model of PD ($P = 0.0024$; **Figure 3C**), and treatment with NBP significantly reduced serum iron induced by rotenone in the rat model of PD ($P = 0.0052$; **Figure 3C**). The expression levels of the three iron-related proteins—TfR, Fpn1, and Ft-L—were examined by western blot after NBP treatment in the rotenone-induced rat model of PD. The results showed that TfR ($P < 0.0001$; **Figure 4A** and **B**) and Ft-L ($P < 0.0001$; **Figure 4A** and **D**) expression significantly increased, while Fpn1 expression was significantly reduced in rats with rotenone-induced PD ($P < 0.0001$; **Figure 4A** and **C**). NBP treatment dramatically reversed the expression of TfR, Fpn1, and Ft-L in the rotenone-induced rat model of PD (TfR: $P = 0.0048$; Fpn1: $P = 0.0027$; Ft-L: $P = 0.0015$; **Figure 4A–D**).

NBP inhibits rotenone-induced oxidative stress, antiferroptosis-related protein expression, and mitochondrial damage in the substantia nigra in a rat model of Parkinson's disease

To further investigate whether the neuroprotective effect of NBP in PD was mediated by a decrease of iron and subsequent reduction in oxidative stress, we tested the effect of NBP on MDA and GSH in the SN, mitochondrial structure, and antiferroptosis-related protein (xCT and GPX4) expression in the rotenone-induced rat model of PD. Our results show that MDA levels increased ($P < 0.0001$; **Figure 5A**) and GSH levels decreased ($P = 0.0448$; **Figure 5A**) after rotenone treatment. NBP inhibited the effects of rotenone on MDA ($P < 0.0001$; **Figure 5A**) and GSH ($P = 0.0011$; **Figure 5B**) levels. In addition, we observed the mitochondrial structure of the SN by transmission electron microscopy and discovered that the mitochondria shrank, the

mitochondrial cristae were reduced, and the outer membrane was ruptured after rotenone exposure in the rat model of PD (**Figure 5C**). As expected, NBP administration alleviated rotenone-induced mitochondrial structural damage and cristae reduction (**Figure 5C**). Because the changes that we observed in the mitochondria were similar to the mitochondrial features observed in ferroptosis, we measured antiferroptosis-related protein expression after NBP treatment in the rat model of PD. GPX4 (P = 0.0005; **Figure 5D** and **E**) and xCT (P = 0.0002; **Figure 5D** and **F**) expressions were significantly decreased in the SN of rotenone-treated rats. Treatment with NBP reversed this effect (GPX4: P = 0.001; xCT: P = 0.0001; **Figure 5D–F**).

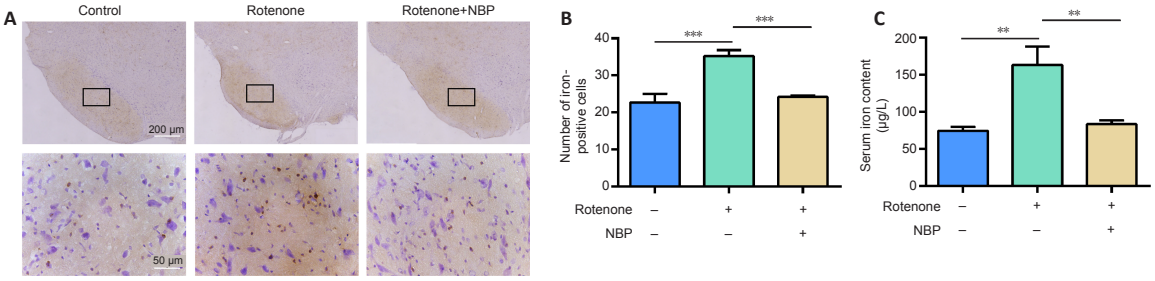

Figure 3 | **NBP decreases the iron content in the substantia nigra and serum in the rotenone-induced rat model of Parkinson's disease.**
(A) Perls' iron staining indicated that rotenone treatment led to an increase in iron deposition in the substantia nigra, while NBP decreased the effects of rotenone on iron deposition in the substantia nigra. Images in the second row are magnifications of the boxed areas in the first row. Scale bars: 200 μm (top) and 50 μm (below). (B) Quantitative results of the number of iron-positive neurons. (C) An inductively coupled plasma mass spectrometer was used to detect iron content in the serum of rotenone-treated rats with or without NBP treatment. All data are shown as the mean ± SEM (n = 5–6 rats per group). $^{**}P < 0.01$, $^{***}P < 0.001$ (one-way analysis of variance followed by Tukey's *post hoc* test). NBP: DL-3-n-butylphthalide.

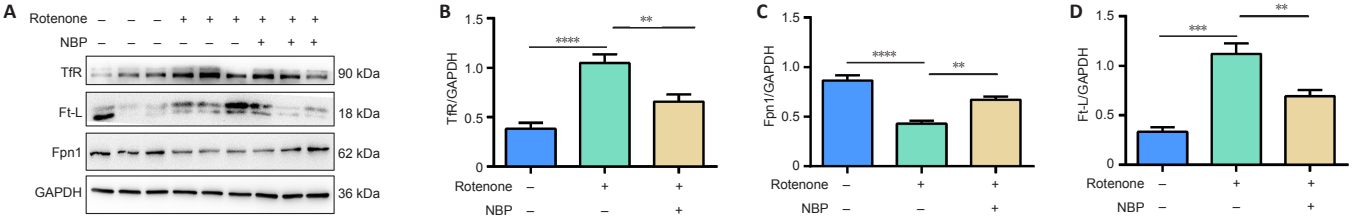

Figure 4 | **NBP reverses iron-related protein expression in the substantia nigra in the rotenone-induced rat model of Parkinson's disease.**
(A) Western blot analysis of the expression of TfR, Ft-L, and Fpn1 in the substantia nigra in the rotenone-induced rat model of Parkinson's disease with or without NBP treatment. (B–D) Quantitative results of TfR (B), Fpn1 (C), and Ft-L (D) expression. All data are shown as the mean ± SEM (n = 5–9 rats per group). $^{**}P < 0.01$, $^{****}P < 0.0001$ (one-way analysis of variance followed by Tukey's *post hoc* test). Fpn 1: Ferroportin 1; Ft-L: ferritin light chain; GAPDH: glyceraldehyde-3-phosphate dehydrogenase; NBP: DL-3-n-butylphthalide; TfR: transferrin receptor.

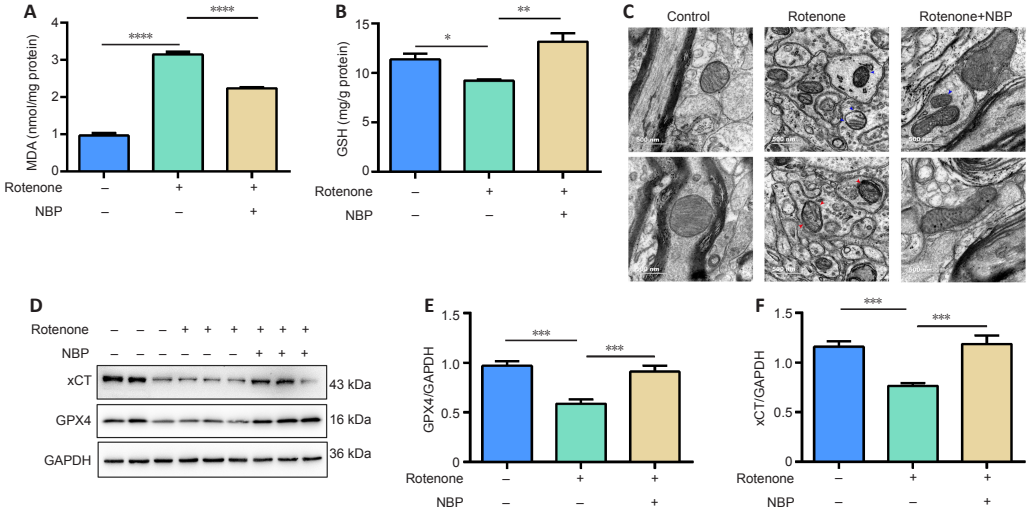

Figure 5 | **NBP reduces oxidative stress and mitochondrial damage and increases xCT and GPX4 expression in the substantia nigra in a rat model of Parkinson's disease.**
(A, B) MDA (A) and GSH (B) levels in the substantia nigra. (C) Mitochondria in the substantia nigra in the rat model of Parkinson's disease with or without NBP treatment were examined using transmission electron microscopy. Mitochondria were intact in the control group; mitochondrial shrinkage was accompanied by increased membrane density and ruptured membrane density. Mitochondrial shrinkage was significantly improved and membrane rupture was alleviated after NBP treatment. Red arrows indicate destruction of the mitochondrial double membrane; blue arrows indicate destruction of the mitochondrial outer membrane. Scale bars: 500 nm. (D) Western blot analysis of the expression of xCT and GPX4 in the substantia nigra in the rotenone-induced rat model of Parkinson's disease with or without NBP treatment. (E, F) Quantitative results of GPX4 (E) and xCT (F) expression. All data are shown as the mean ± SEM (n = 5–10 rats per group). $^{*}P < 0.05$, $^{**}P < 0.01$, $^{***}P < 0.001$, $^{****}P < 0.0001$ (one-way analysis of variance followed by Tukey's *post hoc* test). GAPDH: Glyceraldehyde-3-phosphate dehydrogenase; GSH: glutathione; GPX4: GSH peroxidase 4; MDA: malondialdehyde; NBP: DL-3-n-butylphthalide; xCT: cystine/glutamate antiporter solute carrier family 7 member 11.

Correlations between latency to fall and MDA and GSH levels in the substantia nigra and serum iron levels

We investigated whether NBP rescued motor dysfunction and was correlated with a reduction in oxidative stress in the rat model of PD by analyzing the correlation between the latency to fall and GSH and MDA levels in the SN and the levels of serum iron. As shown in **Figure 6**, the latency to fall was significantly correlated with GSH and MDA levels in the SN and with serum iron levels. A negative correlation was observed between the latency to fall and serum iron levels (r = −0.873, P < 0.0001; **Figure 6A**) and MDA levels (r = −0.809, P < 0.0001; **Figure 6B**). However, the latency to fall was positively correlated with GSH levels (r = 0.798, P = 0.0019; **Figure 6C**).

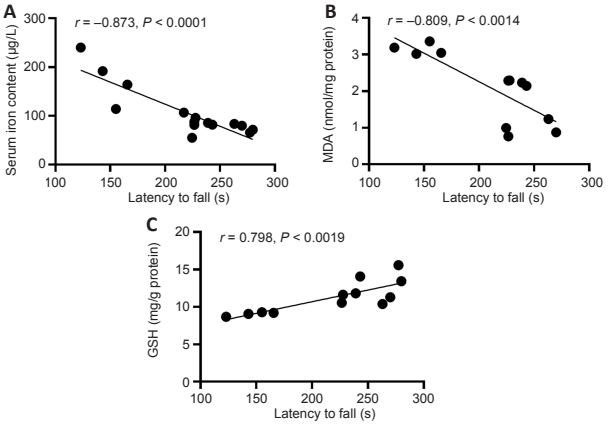

Figure 6 | **Correlation analysis of the relationship between serum iron content, MDA levels, or GSH levels with the latency to fall in a rat model of Parkinson's disease.** (A) Association analysis of serum iron content and latency to fall in the rat model of Parkinson's disease. (B) Association analysis of MDA levels and latency to fall in the rat model of Parkinson's disease. (C) Association analysis of GSH levels and latency to fall in the rat model of Parkinson's disease. Data were analyzed by Pearson's correlation analysis (n = 6–8 rats per group). GSH: Glutathione; MDA: malondialdehyde.

Discussion

Recent evidence indicates that ferroptosis is involved not only in iron deposition and oxidative stress but also in PD development (Dias et al., 2013; Fan et al., 2021; Mahoney-Sánchez et al., 2021; Zhu et al., 2021). Therapeutic strategies to inhibit iron accumulation and ferroptosis may prevent the progression of PD (Zhang et al., 2020). Recently, one study has shown that NBP plays a powerful role in antioxidative stress in various animal models (Liao et al., 2018). Nevertheless, the effects of NBP in a PD model are unclear. Here, we studied the neuroprotective effect and potential mechanism of NBP in a rotenone-induced rat model of PD.

Rotenone is one of the best known neurotoxins that induces PD symptoms (Sherer et al., 2003b; Lin et al., 2008), exhibits selective toxicity to dopaminergic neurons, and produces many characteristics of PD, including degeneration of nigrostriatal dopaminergic neurons and increased α-syn accumulation (Perier et al., 2003; Sherer et al., 2003a). Additionally, rotenone can produce oxidative stress by inhibiting mitochondrial function, reducing intracellular ATP levels, and increasing intracellular ROS levels (Federico et al., 2012). In this study, we used a rotenone-induced PD model to study the therapeutic effects of NBP *in vivo*. Our results demonstrate that NBP prevented rotenone-induced weight loss and ameliorated motor disturbance. In addition, NBP protected against rotenone-induced degeneration of dopaminergic neurons, restored TH-positive neurons, and decreased α-syn expression. Decreased α-syn expression was consistent with previous studies that reported that NBP blocked rotenone-induced oxidative stress in microglia and reduced α-syn accumulation by modulating the Kelch-like ECH-associated protein 1/erythroid 2-related factor 2/heme oxygenase1 signaling pathway (Wu et al., 2019; Luo et al., 2021). Our previous study confirmed that hepcidin, an iron-regulating hormone, suppressed rotenone-induced α-syn expression (Li et al., 2020). These results suggest that NBP may protect dopaminergic neurons against rotenone-induced neurotoxicity by suppressing oxidative stress or reducing iron in the SN. In addition, one study has reported that NBP inhibited rotenone-induced mitochondrial membrane potential production in SH-SY5Y cells, suppressed ROS generation, and alleviated oxidative stress, thereby providing neuroprotection in a PD cell model (Xiong et al., 2012a). NBP also counteracted hydrogen peroxide-induced neural stem cell injury by activating the phosphatidylinositol 3-kinase/protein kinase B pathway (Wang et al., 2018a). Although rotenone-induced iron accumulation is established, it has not yet been reported whether NBP could regulate iron metabolism and affect oxidative stress in the SN of PD models, and the mechanism involved is also unclear.

Many studies have determined that the cellular mechanism of SN iron accumulation leading to PD may be associated with abnormal iron metabolism in the brain (Jiang et al., 2017; Mochizuki et al., 2020). The iron content is significantly increased in the SN and serum of patients with PD and animal models of PD (Berg and Hochstrasser, 2006; Do Van et al., 2016; Liu et al., 2018). Iron homeostasis is maintained by several key iron metabolic proteins, including iron importer TfR, iron exporter Fpn1, and iron storage protein Ft-L. TfR takes up iron via the transferrin-TfR endocytosis pathway, which occurs through recognition and binding with holo-transferrin. Fpn1, which is the only iron exporter identified to date, is located in the cell membrane and is indispensable in maintaining iron homeostasis (Song et al., 2010). Furthermore, Ft-L contains nucleation sites that promote iron-core formation and complete iron preservation. Impairment of the expression of these iron metabolic proteins can destroy the balance of iron homeostasis (Mahoney-Sánchez et al., 2021). Consistent with these roles, iron deposition in the SN in PD was significantly correlated with the expression of iron-associated proteins (Chen et al., 2019a; Mahoney-Sánchez et al., 2021). Therefore, we studied the effect of NBP on the expression of these three iron-related proteins in the SN to elucidate the reason for iron accumulation in a rat model of PD. Numerous experiments have confirmed that the expression levels of TfR and Ft-L are upregulated in the SN in patients with PD and iron accumulation occurs in PD animal models (Wu et al., 2010; Xiong et al., 2012b; Olmedo-Díaz et al., 2017; Xu et al., 2019a; Zhang et al., 2021b). Similarly, we also found that rotenone induced TfR and Ft-L expression and iron accumulation in the SN and serum in the rats used in our current research, which corresponds with our previous measurement of elevated iron content in the serum of patients with PD (Wang et al., 2021). Moreover, we found that rotenone significantly inhibited Fpn1 expression in the rat model of PD. This finding is consistent with other studies that showed a decrease in Fpn1 and a further reduction in iron export from rotenone-induced SH-SY5Y cells (Koziorowski et al., 2007; Zhang et al., 2014). However, NBP treatment reversed the iron accumulation and the iron metabolism-related protein expression changes mentioned above. Our findings suggest that NBP exerts a neuroprotective effect on PD by affecting the expression of proteins involved in iron metabolism, thus inhibiting rotenone-induced SN iron accumulation.

Iron accumulation possibly leads to the initiation of the Fenton reaction, which causes oxidative stress and destruction of dopaminergic neurons in the SN (Koziorowski et al., 2007). Lipid peroxidation is a result of increased oxidative stress and is the cause of ferroptosis, which is directly related to changes in dopaminergic neurons in the SN after rotenone exposure. MDA is a suitable lipid peroxidation marker in the central nervous system (Avcı et al., 2021). In addition, as a reduction substrate for GPX4, GSH is the major antioxidant agent in cells (Armstrong et al., 2002; Dixon et al., 2012; Ursini and Maiorino, 2020). In this study, the increase in MDA and decrease in GSH levels in serum after rotenone treatment indicate that ROS were increased and that lipid peroxidation occurred in the rat model of PD. However, NBP treatment effectively inhibited the oxidative stress induced by rotenone in rats. Because iron accumulation and oxidative stress are the two main factors involved in ferroptosis (Dixon et al., 2012; Stockwell et al., 2017; Jiang et al., 2021), we further observed ferroptosis in the SN in the rat model of PD. Ferroptosis takes part in the pathology of PD (Do Van et al., 2016; Mahoney-Sánchez et al., 2021), and ferroptosis has been reported to be involved in the neuropathological process of rotenone-induced neurotoxicity (Avcı et al., 2021; Sun et al., 2021). In addition, ferroptosis can be effectively inhibited by the iron chelator deferoxamine. The effect of deferoxamine on ferroptosis was similar to that of the ferroptosis inhibitors ferrostatin-1 and liproxstatin-1, which can significantly protect against the loss of dopaminergic neurons in the SN of PD animal models (Do Van et al., 2016; Stockwell et al., 2017).

We hypothesized that NBP might protect dopaminergic neurons from rotenone-induced oxidative damage by iron-dependent ferroptosis. xCT exerts a core effect on antioxidant defense by mediating cystine uptake, driving GSH synthesis, and maintaining cell survival under oxidative stress conditions (Liu et al., 2021), and the selenium-containing enzyme GPX4 is an essential factor in cell redox balance and is an antiferroptotic protein. Its activity depends on the activation of xCT (Ursini and Maiorino, 2020), and we detected changes in the expression of both xCT and GPX4 after NBP treatment. However, NBP inhibited the rotenone-induced impairment of mitochondria and prompted an increase in xCT and GPX4 expression in the SN in the rat model of PD. These data indicate that the reduction in xCT and GPX4 probably causes cells to enter an oxidized state, further aggravating lipid peroxidation and mitochondrial damage and inducing ferroptosis, ultimately prompting dopaminergic neuron loss in a rat model of PD. Nevertheless, NBP can efficiently stop ferroptosis through the upregulation of xCT and GPX4 expression, thereby stopping lipid peroxidation and exerting its neuroprotective effect in a rat model of PD. Our correlation analysis also confirmed that iron accumulation and oxidative stress significantly affected motor disturbance in the rotenone-induced rat model of PD. However, while our study uncovered the effects of NBP on iron metabolism and ferroptosis and alleviated motor disturbance in the rotenone-induced rat model of PD, questions remain to be investigated, including whether NBP first affects iron homeostasis and then affects oxidative stress in rotenone-induced PD or whether it occurs in the reverse order. Whether NBP has the same effect on alleviating motor disturbance via regulation of iron metabolism in other PD models or patients with PD also remains unclear.

In conclusion, in this study, we showed that NBP alleviates motor disturbance in a rat model of PD and protects dopaminergic neurons against rotenone-induced degeneration. NBP reduced iron deposition, suppressed oxidative stress, and inhibited ferroptosis in the SN in a rat model of PD. Our study further confirmed the neuroprotective effect of NBP in treating PD.

Author contributions: *Study design and supervision: QQL, LHS; experiment implementation: CBH, JH; data analysis: HJ, YY, ZZJ, QHJ; manuscript draft and revision: QQL, GHW, LHS. All authors read and approved the final version of the manuscript.*
Conflicts of interest: *No conflict of interest was declared.*

Open peer reviewer: *Nemil N. Bhatt, The University of Texas Medical Branch at Galveston, USA.*

References

Angelova PR, Choi ML, Berezhnov AV, Horrocks MH, Hughes CD, De S, Rodrigues M, Yapom R, Little D, Dolt KS, Kunath T, Devine MJ, Gissen P, Shchepinov MS, Sylantyev S, Pavlov EV, Klenerman D, Abramov AY, Gandhi S (2020) Alpha synuclein aggregation drives ferroptosis: an interplay of iron, calcium and lipid peroxidation. Cell Death Differ 27:2781-2796.

Armstrong JS, Steinauer KK, Hornung B, Irish JM, Lecane P, Birrell GW, Peehl DM, Knox SJ (2002) Role of glutathione depletion and reactive oxygen species generation in apoptotic signaling in a human B lymphoma cell line. Cell Death Differ 9:252-263.

Avcı B, Günaydın C, Güvenç T, Yavuz CK, Kuruca N, Bilge SS (2021) Idebenone ameliorates rotenone-induced parkinson's disease in rats through decreasing lipid peroxidation. Neurochem Res 46:513-522.

Berg D, Hochstrasser H (2006) Iron metabolism in Parkinsonian syndromes. Mov Disord 21:1299-1310.

Betarbet R, Sherer TB, MacKenzie G, Garcia-Osuna M, Panov AV, Greenamyre JT (2000) Chronic systemic pesticide exposure reproduces features of Parkinson's disease. Nat Neurosci 3:1301-1306.

Bloem BR, Okun MS, Klein C (2021) Parkinson's disease. Lancet 397:2284-2303.

Cannon JR, Tapias V, Na HM, Honick AS, Drolet RE, Greenamyre JT (2009) A highly reproducible rotenone model of Parkinson's disease. Neurobiol Dis 34:279-290.

Chen B, Wen X, Jiang H, Wang J, Song N, Xie J (2019a) Interactions between iron and α-synuclein pathology in Parkinson's disease. Free Radic Biol Med 141:253-260.

Chen J, Li Y, Wang L, Zhang Z, Lu D, Lu M, Chopp M (2001) Therapeutic benefit of intravenous administration of bone marrow stromal cells after cerebral ischemia in rats. Stroke 32:1005-1011.

Chen Q, Chen Y, Zhang Y, Wang F, Yu H, Zhang C, Jiang Z, Luo W (2019b) Iron deposition in Parkinson's disease by quantitative susceptibility mapping. BMC Neurosci 20:23.

Chen Y, Jiang M, Li L, Ye M, Yu M, Zhang L, Ge B, Xu W, Wei D (2018) DL-3-n-butylphthalide reduces microglial activation in lipopolysaccharide-induced Parkinson's disease model mice. Mol Med Rep 17:3884-3890.

Deng H, Liu S, Pan D, Jia Y, Ma ZG (2021) Myricetin reduces cytotoxicity by suppressing hepcidin expression in MES23.5 cells. Neural Regen Res 16:1105-1110.

Dias V, Junn E, Mouradian MM (2013) The role of oxidative stress in Parkinson's disease. J Parkinsons Dis 3:461-491.

Ding L, Zhou J, Ye L, Sun Y, Jiang Z, Gan D, Xu L, Luo Q, Wang G (2020) PPAR-γ is critical for HDAC3-mediated control of oligodendrocyte progenitor cell proliferation and differentiation after focal demyelination. Mol Neurobiol 57:4810-4824.

Dixon SJ, Lemberg KM, Lamprecht MR, Skouta R, Zaitsev EM, Gleason CE, Patel DN, Bauer AJ, Cantley AM, Yang WS, Morrison B, 3rd, Stockwell BR (2012) Ferroptosis: an iron-dependent form of nonapoptotic cell death. Cell 149:1060-1072.

Do Van B, Gouel F, Jonneaux A, Timmerman K, Gele P, Petrault M, Bastide M, Laloux C, Moreau C, Bordet R, Devos D, Devedjian JC (2016) Ferroptosis, a newly characterized form of cell death in Parkinson's disease that is regulated by PKC. Neurobiol Dis 94:169-178.

Dorszewska J, Kowalska M, Prendecki M, Piekut T, Kozłowska J, Kozubski W (2021) Oxidative stress factors in Parkinson's disease. Neural Regen Res 16:1383-1391.

Duda JE, Lee VM, Trojanowski JQ (2000) Neuropathology of synuclein aggregates. J Neurosci Res 61:121-127.

Fan BY, Pang YL, Li WX, Zhao CX, Zhang Y, Wang X, Ning GZ, Kong XH, Liu C, Yao X, Feng SQ (2021) Liproxstatin-1 is an effective inhibitor of oligodendrocyte ferroptosis induced by inhibition of glutathione peroxidase 4. Neural Regen Res 16:561-566.

Federico A, Cardaioli E, Da Pozzo P, Formichi P, Gallus GN, Radi E (2012) Mitochondria, oxidative stress and neurodegeneration. J Neurol Sci 322:254-262.

Fujino S, Hamano S, Tomokiyo A, Itoyama T, Hasegawa D, Sugii H, Yoshida S, Washio A, Nozu A, Ono T, Wada N, Kitamura C, Maeda H (2020) Expression and function of dopamine in odontoblasts. J Cell Physiol 235:4376-4387.

Gao M, Yi J, Zhu J, Minikes AM, Monian P, Thompson CB, Jiang X (2019) Role of mitochondria in ferroptosis. Mol Cell 73:354-363.e3.

Gillies GE, Pienaar IS, Vohra S, Qamhawi Z (2014) Sex differences in Parkinson's disease. Front Neuroendocrinol 35:370-384.

Han K, Jin X, Guo X, Cao G, Tian S, Song Y, Zuo Y, Yu P, Gao G, Chang YZ (2021) Nrf2 knockout altered brain iron deposition and mitigated age-related motor dysfunction in aging mice. Free Radic Biol Med 162:592-602.

Heikkila RE, Nicklas WJ, Vyas I, Duvoisin RC (1985) Dopaminergic toxicity of rotenone and the 1-methyl-4-phenylpyridinium ion after their stereotaxic administration to rats: implication for the mechanism of 1-methyl-4-phenyl-1,2,3,6-tetrahydropyridine toxicity. Neurosci Lett 62:389-394.

Jenner P (2001) Parkinson's disease, pesticides and mitochondrial dysfunction. Trends Neurosci 24:245-247.

Jiang H, Wang J, Rogers J, Xie J (2017) Brain iron metabolism dysfunction in Parkinson's disease. Mol Neurobiol 54:3078-3101.

Jiang X, Stockwell BR, Conrad M (2021) Ferroptosis: mechanisms, biology and role in disease. Nat Rev Mol Cell Biol 22:266-282.

Koziorowski D, Friedman A, Arosio P, Santambrogio P, Dziewulska D (2007) ELISA reveals a difference in the structure of substantia nigra ferritin in Parkinson's disease and incidental Lewy body compared to control. Parkinsonism Relat Disord 13:214-218.

Li M, Hu J, Yuan X, Shen L, Zhu L, Luo Q (2020) Hepcidin decreases rotenone-induced α-synuclein accumulation via autophagy in SH-SY5Y cells. Front Mol Neurosci 13:560891.

Liao D, Xiang D, Dang R, Xu P, Wang J, Han W, Fu Y, Yao D, Cao L, Jiang P (2018) Neuroprotective effects of dl-3-n-butylphthalide against doxorubicin-induced neuroinflammation, oxidative stress, endoplasmic reticulum stress, and behavioral changes. Oxid Med Cell Longev 2018:9125601.

Liao SJ, Lin JW, Pei Z, Liu CL, Zeng JS, Huang RX (2009) Enhanced angiogenesis with dl-3n-butylphthalide treatment after focal cerebral ischemia in RHRSP. Brain Res 1289:69-78.

Liaw YF, Leung N, Guan R, Lau GK, Merican I, McCaughan G, Gane E, Kao JH, Omata M (2005) Asian-Pacific consensus statement on the management of chronic hepatitis B: a 2005 update. Liver Int 25:472-489.

Lin CH, Huang JY, Ching CH, Chuang JI (2008) Melatonin reduces the neuronal loss, downregulation of dopamine transporter, and upregulation of D2 receptor in rotenone-induced Parkinsonian rats. J Pineal Res 44:205-213.

Liu LX, Du D, Wang ZQ, Fang Y, Zheng T, Dong YC, Shi QL, Zhao M, Xiao F, Du J (2018) Differences in brain pathological changes between rotenone and 6-hydroxydopamine Parkinson's disease models. Neural Regen Res 13:1276-1280.

Liu X, Zhang Y, Zhuang L, Olszewski K, Gan B (2021) NADPH debt drives redox bankruptcy: SLC7A11/xCT-mediated cystine uptake as a double-edged sword in cellular redox regulation. Genes Dis 8:731-745.

Luo R, Zhu L, Zeng Z, Zhou R, Zhang J, Xiao S, Bi W (2021) Dl-butylphthalide inhibits rotenone-induced oxidative stress in microglia via regulation of the Keap1/Nrf2/HO-1 signaling pathway. Exp Ther Med 21:597.

Mahoney-Sánchez L, Bouchaoui H, Ayton S, Devos D, Duce JA, Devedjian JC (2021) Ferroptosis and its potential role in the physiopathology of Parkinson's disease. Prog Neurobiol 196:101890.

Metz GA, Whishaw IQ (2002) Cortical and subcortical lesions impair skilled walking in the ladder rung walking test: a new task to evaluate fore- and hindlimb stepping, placing, and co-ordination. J Neurosci Methods 115:169-179.

Mochizuki H, Choong CJ, Baba K (2020) Parkinson's disease and iron. J Neural Transm (Vienna) 127:181-187.

National Research Council (US) Committee for the Update of the Guide for the Care and Use of Laboratory Animals (2011) Guide for the Care and Use of Laboratory Animals, 8th Edition. Washington (DC): National Academies Press (US).

Olmedo-Díaz S, Estévez-Silva H, Orädd G, Af Bjerkén S, Marcellino D, Virel A (2017) An altered blood-brain barrier contributes to brain iron accumulation and neuroinflammation in the 6-OHDA rat model of Parkinson's disease. Neuroscience 362:141-151.

Perier C, Bové J, Vila M, Przedborski S (2003) The rotenone model of Parkinson's disease. Trends Neurosci 26:345-346.

Risold PY, Swanson LW (1997) Chemoarchitecture of the rat lateral septal nucleus. Brain Res Brain Res Rev 24:91-113.

Schneider CA, Rasband WS, Eliceiri KW (2012) NIH Image to ImageJ: 25 years of image analysis. Nat Methods 9:671-675.

Sherer TB, Kim JH, Betarbet R, Greenamyre JT (2003a) Subcutaneous rotenone exposure causes highly selective dopaminergic degeneration and alpha-synuclein aggregation. Exp Neurol 179:9-16.

Sherer TB, Betarbet R, Testa CM, Seo BB, Richardson JR, Kim JH, Miller GW, Yagi T, Matsuno-Yagi A, Greenamyre JT (2003b) Mechanism of toxicity in rotenone models of Parkinson's disease. J Neurosci 23:10756-10764.

Song N, Wang J, Jiang H, Xie J (2010) Ferroportin 1 but not hephaestin contributes to iron accumulation in a cell model of Parkinson's disease. Free Radic Biol Med 48:332-341.

Spillantini MG, Schmidt ML, Lee VM, Trojanowski JQ, Jakes R, Goedert M (1997) Alpha-synuclein in Lewy bodies. Nature 388:839-840.

Stockwell BR, Friedmann Angeli JP, Bayir H, Bush AI, Conrad M, Dixon SJ, Fulda S, Gascón S, Hatzios SK, Kagan VE, Noel K, Jiang X, Linkermann A, Murphy ME, Overholtzer M, Oyagi A, Pagnussat GC, Park J, Ran Q, Rosenfeld CS, et al. (2017) Ferroptosis: a regulated cell death nexus linking metabolism, redox biology, and disease. Cell 171:273-285.

Sun WY, Tyurin VA, Mikulska-Ruminska K, Shrivastava IH, Anthonymuthu TS, Zhai YJ, Pan MH, Gong HB, Lu DH, Sun J, Duan WJ, Korolev S, Abramov AY, Angelova PR, Miller I, Beharier O, Mao GW, Dar HH, Kapralov AA, Amoscato AA, et al. (2021) Phospholipase iPLA(2)β averts ferroptosis by eliminating a redox lipid death signal. Nat Chem Biol 17:465-476.

Tian X, He W, Yang R, Liu Y (2017) Dl-3-n-butylphthalide protects the heart against ischemic injury and H9c2 cardiomyoblasts against oxidative stress: involvement of mitochondrial function and biogenesis. J Biomed Sci 24:38.

Ursini F, Maiorino M (2020) Lipid peroxidation and ferroptosis: The role of GSH and GPx4. Free Radic Biol Med 152:175-185.

von Wrangel C, Schwabe K, John N, Krauss JK, Alam M (2015) The rotenone-induced rat model of Parkinson's disease: behavioral and electrophysiological findings. Behav Brain Res 279:52-61.

Wang J, Bi M, Xie J (2015) Ceruloplasmin is involved in the nigral iron accumulation of 6-OHDA-lesioned rats. Cell Mol Neurobiol 35:661-668.

Wang S, Huang L, Zhang Y, Peng Y, Wang X, Peng Y (2018a) Protective effects of L-3-n-butylphthalide against H(2)O(2)-induced injury in neural stem cells by activation of PI3K/Akt and Mash1 pathway. Neuroscience 393:164-174.

Wang S, Ma F, Huang L, Zhang Y, Peng Y, Xing C, Feng Y, Wang X, Peng Y (2018b) Dl-3-n-butylphthalide (NBP): a promising therapeutic agent for ischemic stroke. CNS Neurol Disord Drug Targets 17:338-347.

Wang Z, Liu Y, Gao Z, Shen L (2021) The relationship between levels of serum metal ions and Parkinson's disease. Clin Lab 67.

Wu CT, Deng JS, Huang WC, Shieh PC, Chung MI, Huang GJ (2019) Salvianolic acid c against acetaminophen-induced acute liver injury by attenuating inflammation, oxidative stress, and apoptosis through inhibition of the Keap1/Nrf2/HO-1 signaling. Oxid Med Cell Longev 2019:9056845.

Wu Y, Li X, Xie W, Jankovic J, Le W, Pan T (2010) Neuroprotection of deferoxamine on rotenone-induced injury via accumulation of HIF-1 alpha and induction of autophagy in SH-SY5Y cells. Neurochem Int 57:198-205.

Xiong N, Huang J, Chen C, Zhao Y, Zhang Z, Jia M, Zhang Z, Hou L, Yang H, Cao X, Liang Z, Zhang Y, Sun S, Lin Z, Wang T (2012a) Dl-3-n-butylphthalide, a natural antioxidant, protects dopamine neurons in rotenone models for Parkinson's disease. Neurobiol Aging 33:1777-1791.

Xiong P, Chen X, Guo C, Zhang N, Ma B (2012b) Baicalin and deferoxamine alleviate iron accumulation in different brain regions of Parkinson's disease rats. Neural Regen Res 7:2092-2098.

Xu SF, Zhang YH, Wang S, Pang ZQ, Fan YG, Li JY, Wang ZY, Guo C (2019a) Lactoferrin ameliorates dopaminergic neurodegeneration and motor deficits in MPTP-treated mice. Redox Biol 21:101090.

Xu ZQ, Zhou Y, Shao BZ, Zhang JJ, Liu C (2019b) A systematic review of neuroprotective efficacy and safety of DL-3-N-butylphthalide in ischemic stroke. Am J Chin Med 47:507-525.

Zhang D, Li S, Hou L, Jing L, Ruan Z, Peng B, Zhang X, Hong JS, Zhao J, Wang Q (2021a) Microglial activation contributes to cognitive impairments in rotenone-induced mouse Parkinson's disease model. J Neuroinflammation 18:4.

Zhang N, Yu X, Xie J, Xu H (2021b) New insights into the role of ferritin in iron homeostasis and neurodegenerative diseases. Mol Neurobiol 58:2812-2823.

Zhang P, Chen L, Zhao Q, Du X, Bi M, Li Y, Jiao Q, Jiang H (2020) Ferroptosis was more initial in cell death caused by iron overload and its underlying mechanism in Parkinson's disease. Free Radic Biol Med 152:227-234.

Zhang Z, Hou L, Song JL, Song N, Sun YJ, Lin X, Wang XL, Zhang FZ, Ge YL (2014) Pro-inflammatory cytokine-mediated ferroportin down-regulation contributes to the nigral iron accumulation in lipopolysaccharide-induced Parkinsonian models. Neuroscience 257:20-30.

Zhou PT, Wang LP, Qu MJ, Shen H, Zheng HR, Deng LD, Ma YY, Wang YY, Wang YT, Tang YH, Tian HL, Zhang ZJ, Yang GY (2019) Dl-3-N-butylphthalide promotes angiogenesis and upregulates sonic hedgehog expression after cerebral ischemia in rats. CNS Neurosci Ther 25:748-758.

Zhu HY, He QJ, Yang B, Cao J (2021) Beyond iron deposition: making sense of the latest evidence on ferroptosis in Parkinson's disease. Acta Pharmacol Sin 42:1379-1381.

P-Reviewer: Bhatt NN; C-Editor: Zhao M; S-Editors: Yu J, Li CH; L-Editors: Yu J, Song LP; T-Editor: Jia Y